THE MAGNETIC FIELD IMPACT ON ACCRETION RATE IN A PROTOPLANETARY DISK

M.M. Kuksa

National Research Nuclear University "MEPHI"
Obninsk Institute of Nuclear Power Engineering
Obninsk, Russia, max@kuksa.ru

ABSTRACT. Recent observations are the evidence of a large-scale magnetic field in discs around classical T Tauri stars. A model of the axisymmetric thin protoplanetary disk in a global magnetic field is considered. A compressible magnetohydrodynamic set of equations is solved by using the explicit numerical method. The influence of a magnetic field and various turbulent kinematic and magnetic viscosity coefficients on the accretion rate in the disk is investigated.

Key words: magnetohydrodynamics; protoplanetary disk: accretion rate

1. Introduction

The origin of an angular momentum transport remains one of the central problems in the accretion disk theory, as molecular viscosity cannot provide the necessary accretion rate.

N.I.Shakura and R.A.Sunyaev (1973), D.Lynden-Bell and J.Pringle (1974) had noted that turbulence would cause enhanced viscosity. Several angular momentum transport mechanisms were offered such as convection, nonlinear hydrodynamic instability, gravitational instability and perturbations caused by external influences. However neither of them can transfer angular momentum for required time.

Progress has been made with the discovery of magnetorotational instability (MRI). MRI, originally studied by E.P.Velikhov (1959) and S.Chandrasekhar (1961), was applied to astrophysical disks by S.Balbus and J.Hawley (1991, 1992). MRI arises in a differentially rotating disk in the presence of a weak magnetic field. Numerical simulations (Hawley, Gammie, Balbus, 1995, 1996) have shown that MRI led to turbulence, transported the angular momentum outward and acted as a hydromagnetic dynamo, i.e. sustained magnetic field in the presence of dissipation.

It has been shown that in the so-called dead zone between active layers in protoplanetary disks, MRI cannot operate (Gammie, 1996). However the account of non-ideal effects such as Hall effect and ambipolar diffusion resulted in changing the stability and the saturation of MRI in weakly-ionized protoplanetary disks (Balbus, Terquem, 2001; Wardle, 1999, 2007).

In recent years direct measurements have shown a clear evidence of the magnetic field in protostellar disks. The existence of a significant azimuthal magnetic field of about 1 kG has been confirmed by observations around

FU Orionis in the innermost regions of its accretion disk (Donati et al., 2005). Furthermore observations and analysis of a magnetic field on the surface of classical T Tauri stars suggest a strong octopolar field (~1.2 kG) and a smaller dipolar field (~0.35 kG) (Donati et al., 2007).

It should be noted that MRI is stable in a strong magnetic field and generation of a large-scale magnetic field by MRI is not observed (Brandenburg, Nordlund, Stein, 1995; Hawley, 2001).

Recently F.Ebrahimi and S.Prager (2011) have explored the possibility of an angular momentum transport in disks by tearing instabilities of plasma, which can exist in strongly magnetized regions, for instance, coronas. The effectiveness of it is equivalent to $\alpha \sim 0.01$ by the authors' estimation.

Thus magnetic fields play an important role in accretion all across the disk. So it is reasonably to examine the influence of a magnetic field on the accretion rate in a global scale. This paper studies the 2D evolution model of a protoplanetary disk in a large-scale magnetic field.

2. Model

The thin gaseous disk evolution is described by the following set of equations

$$\begin{cases} \dfrac{\partial \Sigma}{\partial t} = -\boldsymbol{u} \cdot \nabla \Sigma - \Sigma \nabla \cdot \boldsymbol{u} \\[2mm] \dfrac{\partial \boldsymbol{u}}{\partial t} = -(\boldsymbol{u} \cdot \nabla) \cdot \boldsymbol{u} - c_s^2 \nabla \ln \Sigma - \dfrac{GM_\odot}{r^2} + \\[2mm] \quad + \nu \left(\nabla^2 \boldsymbol{u} + \dfrac{1}{3} \nabla \nabla \cdot \boldsymbol{u} + 2S \cdot \dfrac{\nabla \Sigma}{\Sigma} \right) + \dfrac{(\nabla \times \boldsymbol{B}) \times \boldsymbol{B}}{4\pi \Sigma} \\[2mm] c_s^2 = c_{s0}^2 \exp \left[(\gamma - 1) \ln \dfrac{\Sigma}{\Sigma_0} \right] \\[2mm] \dfrac{\partial \boldsymbol{A}}{\partial t} = \boldsymbol{u} \times \boldsymbol{B} + \eta \Delta \boldsymbol{A} \\[2mm] \nabla \cdot \boldsymbol{B} = 0 \end{cases}$$

where t is the time, r is the radial distance, Σ and Σ_0 are the surface density and its initial value, respectively, $\boldsymbol{u}$ is the velocity vector, c_s and c_{s0} are the sound speed and its initial value, respectively, $\boldsymbol{A}$ is the vector potential, $\boldsymbol{B}$ is the magnetic induction vector, G is the gravitation constant, $M_\odot$ is the protosun mass, which equals to the modern solar mass, ν is the turbulent kinematic viscosity, η is the turbulent magnetic viscosity, $\gamma = 5/3$ is the adiabatic index and traceless strain rate tensor

$$S = \frac{1}{2}\left(\nabla \boldsymbol{u} + (\nabla \boldsymbol{u})^T\right) - \frac{1}{3}\nabla \cdot \boldsymbol{u}.$$

The pressure gradient acceleration in the equation of motion is expressed in terms of squared sound speed and logarithmic surface density gradient

$$\frac{\nabla p}{\Sigma} = \frac{\nabla(\Sigma c_s^2)}{\Sigma \gamma} = c_s^2 \nabla \ln \Sigma.$$

The turbulent kinematic viscosity is defined according to the standard prescription (Shakura, Sunyaev, 1973)

$$\nu = \alpha \frac{c_s^2}{\Omega},$$

where Ω is the angular velocity, α is the dimensionless parameter.

The turbulent magnetic viscosity according to (Campbell, 1997) may be specified similarly to the former one with the parameter β

$$\eta = \beta \frac{c_s^2}{\Omega}.$$

The resulting magnetic field is
$$\boldsymbol{B} = \boldsymbol{B}_d + \boldsymbol{B}_{ext},$$

where $\boldsymbol{B}_d = \nabla \times \boldsymbol{A}$ is the proper disk magnetic field, $\boldsymbol{B}_{ext} = (0,0,B_{ext,z})$ is the external magnetic field with a vertical component only.

The disk model is considered in polar coordinates (r, φ). The origin of coordinates is the center of the star and the coordinate plane coincides with the equatorial plane of a disk. The disk is suggested to be axisymmetric. The modeling region extends from 0.5 to 1.5 AU.

3. Numerical method

Numerical simulations are performed with the help of Pencil Code (Brandenburg, 2003). The modeling area is covered by a grid with $n = 1200$ points and constant spacing Δr. Spatial derivatives are approximated by the sixth order finite differences

$$f_i' = \frac{-f_{i-3} + 9f_{i-2} - 45f_{i-1} + 45f_{i+1} - 9f_{i+2} + f_{i+3}}{60\Delta r},$$

$$f_i'' = \frac{2(f_{i+3} + f_{i-3}) - 27(f_{i+2} + f_{i-2}) + 270(f_{i+1} + f_{i-1}) - 490f_i}{180(\Delta r)^2},$$

where $i = 1,...,n$. Also the continuity equation is complemented by an upwinding term.

A time derivative is calculated by the third order explicit Runge-Kutta method. The time step Δt is derived from the Courant–Friedrichs–Lewy condition.

At the initial time moment the surface density is $\Sigma_0 = 2000$ g/cm^2, the sound speed $c_{s0} = 1.5 \cdot 10^5$ cm/s, the

azimuthal velocity has Keplerian profile $u_{\varphi 0} = \sqrt{GM/r}$, the radial velocity and the vector potential in the disk are zero.

At the left edge (nearer to the star) and at the right edge (farther from the star) the grid is appended by three boundary points. Thus the general number of points is $N = n + 6$. At the each time step the boundary conditions are applied as in Table 1.

Table 1: Boundary conditions

Physical quantity	Boundary values	
	at the left in r_{-2}, r_{-1}, r_0	at the right in $r_{n+1}, r_{n+2}, r_{n+3}$
Surface density	Copy of $\Sigma(r_1)$	2000 g/cm^2
Radial velocity	Copy of $u_r(r_1)$	Copy of $u_r(r_n)$
Azimuthal velocity	Asymmetric extrapolation*	Keplerian $\sqrt{GM/r_i}$
Vector potential	Asymmetric extrapolation*	Asymmetric extrapolation**
* $V(r_{1-i}) = 2V(r_1) - V(r_{1+i})$		
** $V(r_{n+i}) = 2V(r_n) - V(r_{n-i})$,		
$i = 1, 2, 3$, V – extrapolated quantity		

4. Results

A series of numerical tests was performed with the model for various model parameters such as external magnetic field, turbulent kinematic and magnetic viscosity coefficients. Time-average values of surface density, radial velocity, proper disk magnetic field (vertical component) and the accretion rate $\langle M'\rangle$ are obtained at the distance of 0.5 AU from the star and presented in Table 2.

The characteristic property of model evolution is a mass transfer to the star side, i.e. accretion. There are neither artificial inflow nor outflow of mass in simulations, but there are only preconditions for it. The calculated accretion rate of about 10^{-7} $M\odot$/year is the result of "free" (as far as boundary conditions allow) model evolution and agrees with observations of classical T Tauri stars.

Independently of mass source density (fixed density at the outer boundary) the turbulent kinematic viscosity provides only finite radial velocity of transfer. In addition the more viscosity the more is radial velocity magnitude (see models #1, #2 in Table 2).

In the presence of an external magnetic field and equal turbulent kinematic and magnetic viscosities the disk obtains a proper magnetic field. The initial unstable state excites oscillations of the proper magnetic field and

Table 2: Model parameters and evolution results

#	Parameters			Calculated values at 0.5 AU				Model behavior
	$B_{ext,z}$, G	α	β	$\langle\Sigma\rangle$, g/cm^2	$\langle u_r\rangle$, cm/s	$\langle B_{d,z}\rangle$, G	$\langle M'\rangle$, 10^{-7} $M\odot$/ year	
1	–	0,01	–	1538	−394	0	4,4	Steady state
2	–	0,001	–	1453	−44	0	0,3	Steady state
3	1	0,01	0,01	1539	−394	−1	4,5	Decaying oscillations, steady state
4	1	0,001	0,01	1455	−43	−1	0,3	Decaying oscillations, steady state
5	−1	0,01	0,01	1539	−395	1	4,5	Decaying oscillations, steady state
6	0,001	0,01	0,001	–	–	–	–	Increasing oscillations, scheme instability
7	−1	0,01	0,001	–	–	–	–	Increasing oscillations, scheme instability
8	−1	0,01	0,05	1359↘	−360↗	−41↘	3,7↘	Increase of $|B_{d,z}|$, scheme instability
9	0,001	0,01	0,1	1070	−359	58	2,8	Increase of $|B_{d,z}|$, steady state

Evolution at 0.5 AU from 0 to 150000 revs, statistics from 5000 to 150000 revs
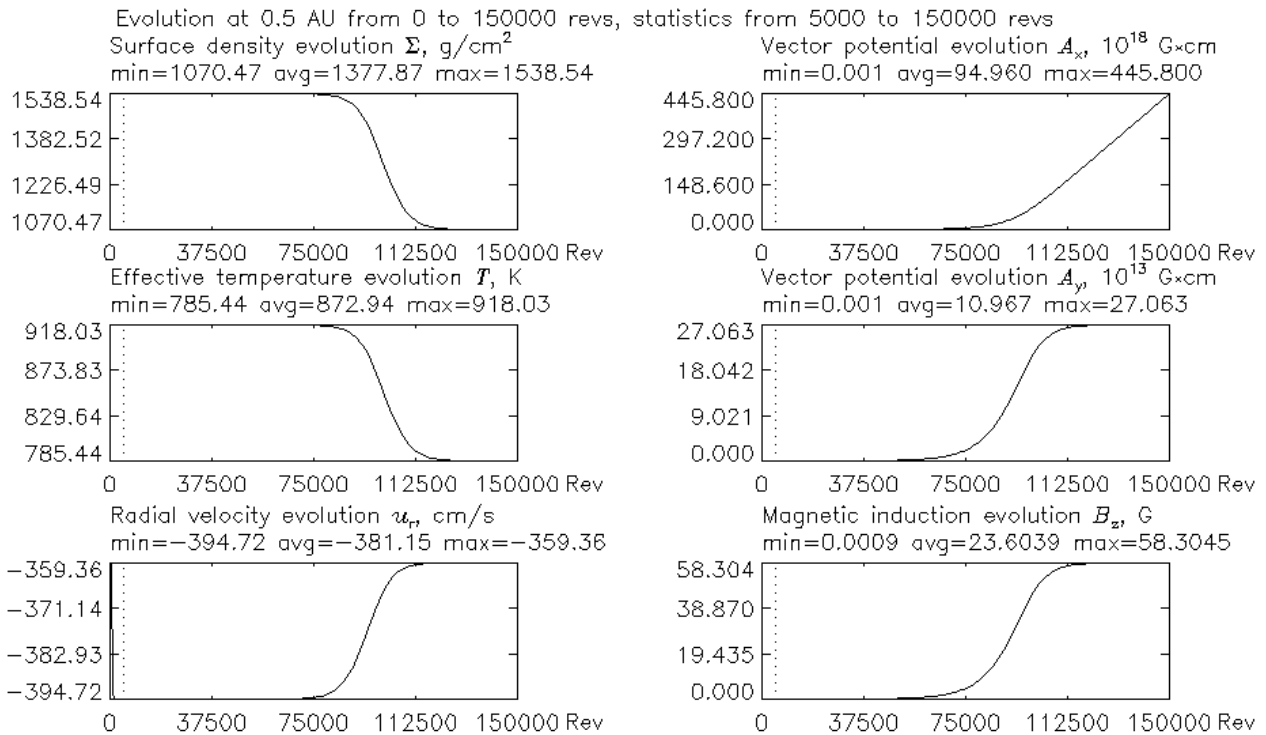
Figure 1: Evolution of the model #9. Revolutions about the star are marked at the abscissa.

velocities in the disk. However in the long run the model comes to steady state, when the proper magnetic field is equal in magnitude and opposite in sign to the external field. The proper disk magnetic field of the strength of 1 G doesn't influence the accretion rate (see #3, #5). The proper magnetic field is decaying when the external field is "turned off".

In the presence of an external magnetic field and different turbulent kinematic and magnetic viscosities there are several scenarios:

1) $\beta = 10\alpha$ and $\beta \leq 0,01$ – decaying oscillations lead to the steady state, in which the magnetic field doesn't affect the accretion rate (see #4).

2) $\beta = 0,1\alpha$ and $\beta \leq 0,001$ – increasing oscillations of a proper magnetic field and velocities in the disk lead to numerical instability, and independently of the magnetic field magnitude and orientation in a vertical direction (see #6, #7).

3) $\beta = 5\alpha$, $\alpha = 0,01$ and $|B_{\text{ext,z}}| = 1$ – increasing magnitude of the proper magnetic field is accompanied by the accretion rate reduction, then numerical instability occurs (see #8). So the model with the lower external field has been examined.

4) $\beta = 10\alpha$, $\alpha = 0,01$ and $|B_{\text{ext,z}}| = 0,001$ – increasing of the proper magnetic field as before is accompanied by the accretion rate reduction, but leads to the steady state (see #9 and Figure 1).

Thus in our simulations the growth of the proper magnetic field magnitude in a disk reduces the radial velocity in the absolute value and hence brings down the accretion rate (see #8, #9).

If new observational data evidence the existence of strong magnetic fields in protoplanetary disks it is reasonable to take the account of magnetohydrodynamic instabilities capable to operate under such conditions, for instance, tearing instabilities.

References

Balbus S.A., Hawley J. F.: 1991, *ApJ.*, **376**, 214.
Balbus S.A., Hawley J. F.: 1991, *ApJ.*, **376**, 223.
Balbus S.A., Hawley J. F.: 1992, *ApJ.*, **400**, 595.
Balbus S.A., Hawley J. F.: 1992, *ApJ.*, **400**, 610.
Balbus S.A., Terquem C.: 2001, *ApJ.*, **552**, 235.
Brandenburg A.: 2003, *The Fluid Mechanics of Astrophysics and Geophysics*, **9**, 269.
Brandenburg A., Nordlund A., Stein R. F., Torkelsson U.: 1995, *ApJ.*, **446**, 741.
Campbell C.G.: 1997, *Magnetohydrodynamics in binary stars*, 306 p.
Chandrasekhar S.: 1961, *Hydrodynamic and hydro-magnetic stability*, 654 p.
Donati J.-F., Paletou F., Bouvier J. et al.: 2005, *Nature*, **438**, 466.
Donati J.-F., Jardine M.M., Gregory S.G. et al.: 2007, *Mon. Not. R. Astron.* Soc., **380**, 1297.
Ebrahimi F., Prager S.C.: 2011, *ApJ.*, **743**, 192.
Gammie C.F.: 1996, *ApJ.*, **457**, 355.
Hawley J.F., Gammie C.F., Balbus S.A.: 1995, *ApJ.*, **440**, 742.
Hawley J.F., Gammie C.F., Balbus S.A.: 1996, *ApJ.*, **464**, 690.
Hawley J.F.: 2001, *ApJ.*, **554**, 534.
Lynden-Bell D., Pringle J.E.: 1974, *Mon. Not. R. Astron. Soc.*, **168**, 603.
Shakura N.I., Sunyaev R.A.: 1973, *A&A.*, **24**, 337.
Velikhov E.P.: 1959, *Sov. Phys. JETP.*, **9**, 995.
Wardle M.: 1999, *Mon. Not. R. Astron. Soc.*, **307**, 849.
Wardle M.: 2007, *Astrophys. and Space Science*, **311**, 35.